where $|F_o|$ and $|F_c|$ are the observed and calculated structure factor amplitudes. Atomic scattering factors and complex anomalous dispersion corrections were taken from refs 32–34. Agreement factors are defined as $R_1 = \sum||F_o| - |F_c||/\sum|F_o|$ and $R_2 = [\sum w||F_o| - |F_c||^2/\sum w|F_o|^2]^{1/2}$. The goodness-of-fit is defined as GOF = $[\sum w(|F_o| - |F_c|)^2/(N_o - N_p)]^{1/2}$, where N_o and N_p are the number of observations and parameters.

The coordinates of the tantalum and silicon atoms were obtained from three-dimensional Patterson maps. Analysis of subsequent difference Fourier maps led to the location of the remaining heavy atoms. Refinement using anisotropic Gaussian amplitudes followed by difference Fourier synthesis resulted in the location of the silicon hydrogens, most of the Cp hydrogens, and at least one hydrogen on each methyl group. All remaining hydrogen atoms were placed at idealized locations (D(C–H) = 0.95 Å) by using the program HYDRO.[31] Final refinement included anisotropic Gaussian amplitudes for all non-hydrogen atoms and fixed positions and fixed isotropic parameters for the hydrogen atoms. Final agreement factors are listed in Table I. Final positional parameters, Gaussian amplitudes, and structure factor amplitudes for **3** and **4a** are included in the supplementary material.

Acknowledgment. Financial support of this work by the National Science Foundation (Grant CHE-8808161) is gratefully acknowledged. We are also grateful to Dr. Terry Rathman of the Lithium Corporation of America for a generous gift of silanes. D.H.B. also thanks the University of Pennsylvania Natural Science Association for a Young Faculty Award.

Supplementary Material Available: Tables of positional parameters and their estimated standard deviations, anisotropic thermal parameters, and intramolecular distances and angles (16 pages); tables of final structure factor amplitudes for **3** and **4a** (36 pages). Ordering information is given on any current masthead page.

(32) *International Tables for X-Ray Crystallography*; Kynoch: Birmingham, England, 1974; Vol. IV, Table 2.2B.

(33) Stewart, R. F.; Davidson, E. R.; Simpson, W. T. *J. Chem. Phys.* **1965**, *42*, 3175–3187.

(34) *International Tables for X-Ray Crystallography*; Kynoch: Birmingham, England, 1974; Vol. IV, Table 2.3.1.

Open and Half-Open Ruthenocenes and Osmocenes: Protonations, Structures, and Reactions with Carbonyl and Phosphine Ligands

Timothy D. Newbound,[1] Lothar Stahl,[1] Manfred L. Ziegler,*[,2] and Richard D. Ernst*[,1]

Department of Chemistry, University of Utah, Salt Lake City, Utah 84112,
and Institut für Anorganische Chemie der Universität Heidelberg, D-6900 Heidelberg 1, West Germany

Received March 22, 1990

The synthesis of a protonated "open ruthenocene", "$HRu(2,4\text{-}C_7H_{11})_2{}^+BF_4{}^-$", is reported, as well as its osmium analogue. The addition of 1 equiv of CO or $P(OMe)_3$ leads to the formation of mono(ligand) adducts, during which one of the pentadienyl ligands and the hydride ligand combine to yield an η^4-2,4-dimethylpentadiene complex, in accord with the formulation of "$HRu(2,4\text{-}C_7H_{11})_2{}^+$" as an agostic species. The addition of 2 equiv of a second ligand to the monoadducts then brings about the removal of the diene ligand, allowing isolation of $Ru(2,4\text{-}C_7H_{11})(CO)_2(PEt_3)^+$ and $Ru(2,4\text{-}C_7H_{11})(CO)(PEt_3)_2{}^+$, as well as symmetric complexes such as $Ru(2,4\text{-}C_7H_{11})(L)_3{}^+$ (L = CO, $P(OMe)_3$, PMe_3). X-ray diffraction studies are reported for several of these compounds. Crystals of $Os(C_5H_5)(2,4\text{-}C_7H_{11})$ are isomorphous with the iron and ruthenium analogues, being orthorhombic, space group *Pnma* (No. 62), with a = 5.900 (2) Å, b = 13.089 (7) Å, c = 13.503 (6) Å, and Z = 4. The structure was refined to discrepancy indices of R = 0.043 and R_W = 0.044 for 1170 reflections having $I > 2.5\sigma(I)$ and revealed similar Os–C distances for the open and closed dienyl ligands. Crystals of $Ru(2,4\text{-}C_7H_{11})(\eta^4\text{-}2,4\text{-}C_7H_{12})(CO)^+BF_4{}^-$ are monoclinic, space group $P2_1/n$ (No. 14), with a = 8.436 (6) Å, b = 13.818 (4) Å, c = 15.199 (9) Å, β = 104.72 (5)°, and Z = 4. The structure was refined to discrepancy indices of R = 0.053 and R_W = 0.046 for 2337 reflections having $I > 2.5\sigma(I)$. The general structure involves the diene and dienyl fragments having their open edges essentially eclipsed, with the carbonyl ligand being situated between these open edges. Crystals of $Ru(2,4\text{-}C_7H_{11})(CO)_2(PEt_3)^+BF_4{}^-$ are monoclinic, space group $P2_1/m$ (No. 11), with a = 8.863 (2) Å, b = 12.246 (2) Å, c = 9.801 (2) Å, β = 112.98 (2)°, and Z = 2. The structure was refined to discrepancy indices of R = 0.037 and R_W = 0.032 for 2337 reflections having $I > 2.5\sigma(I)$. The structure may be regarded as symmetric, with the phosphine ligand located under the open edge of the dienyl ligand and the two carbonyl ligands located under the formally uncharged pentadienyl carbon atoms in the 2- and 4-positions. The carbonyl ligands are crystallographically equivalent, being related to one another by a mirror plane that bisects the dienyl and phosphine ligands. Crystals of $Ru(2,4\text{-}C_7H_{11})(CO)(PEt_3)_2{}^+BF_4{}^-$, as an apparent ethanol solvate, are monoclinic, space group $P2_1/n$ (No. 14), with a = 10.809 (3) Å, b = 27.134 (7) Å, c = 10.879 (3) Å, β = 115.40 (2)°, and Z = 4. The structure was refined to discrepancy indices of R = 0.067 and R_W = 0.054 for 1578 reflections having $I > 2.5\sigma(I)$. This structure may be regarded as unsymmetric, being related to the previous one by replacement of one carbonyl ligand under a formally uncharged carbon atom by the second PEt_3 molecule.

Pentadienyl ligands have recently been attracting growing attention.[3] To a large extent, this has occurred as a result of pentadienyl's ability to bond to transition metals very favorably, in some cases better than cyclo-

---

(1) University of Utah.

(2) Universität Heidelberg.

0276-7333/90/2309-2962$02.50/0 © 1990 American Chemical Society

pentadienyl, while still retaining high degrees of reactivity in potentially useful naked metal and coupling reactions involving unsaturated organic molecules.[4] Additionally, the metal–dienyl complexes generally seem to be much more susceptible to protonation[5] than the metallocenes, for which very acidic conditions are required. As such protonations should allow for the subsequent selective removal of a pentadienyl ligand, they offer some potentially useful routes to the syntheses of new organometallic compounds. Herein we report on the protonations of the open ruthenocene and open osmocene complexes $M(2,4\text{-}C_7H_{11})_2$ and the utilization of the protonated species for the preparations of a variety of mono(dienyl)ruthenium compounds.

Experimental Section

All operations involving organometallics were carried out under a nitrogen atmosphere in a prepurified Schlenk apparatus or in a glovebox. Nonaqueous solvents were thoroughly dried and deoxygenated in a manner appropriate to each and were distilled immediately before use.[6] Elemental analyses were performed by Desert Analytics Laboratories.

Spectroscopic Studies. Infrared spectra were recorded with a Perkin-Elmer 298 spectrophotometer. Mulls were prepared in a glovebox with dry, degassed Nujol. ^1H and ^{13}C nuclear magnetic resonance spectra were recorded in benzene-d_6 or toluene-d_8 on Varian EM-390, SC-300, and XL-300 spectrometers. Mass spectra (70 eV) were recorded on a VG Micromass 7070 double-focusing high-resolution mass spectrometer with the VG Data System 2000. Except for the parent fragment, peaks are only quoted if their relative intensity is at least 10% of the major peak.

(η^5-2,4-Dimethylpentadienyl)(η^6-2,4-dimethylpentadiene)ruthenium Tetrafluoroborate, $[Ru(\eta^5\text{-}2,4\text{-}C_7H_{11})(\eta^6\text{-}2,4\text{-}C_7H_{12})]^+BF_4^-$ ("$HRu(2,4\text{-}C_7H_{11})_2^{+}$"). In a 200-mL, two-neck flask equipped with a nitrogen inlet and stirring bar, 300 mg (1.06 mmol) of bis(2,4-dimethylpentadienyl)ruthenium[7] is dissolved in ca. 30 mL of diethyl ether to give a light yellow solution. The flask is then cooled to −78 °C, and with stirring, 4.7 mL of 0.22 M $HBF_4{\cdot}Et_2O$ is added dropwise by syringe over ca. 1 min. A light yellow solid precipitates immediately following the addition of the tetrafluoroboric acid. While it is stirred, the reaction mixture is warmed up slowly to room temperature. Following removal of the stirrer a light yellow, flocculent precipitate settles out of the colorless liquid. The supernatant is removed by syringe, and the solid is washed with ether and hexane in this order. The yield of this reaction is quantitative; due to lack of complete recovery of the solid, however, the isolated yield is 380 mg (94%, mp 159–161 °C). The yellow product obtained in this manner is analytically pure and may be used for NMR and IR studies. Single crystals of the title compound are obtained by dissolving the solid in a minimum amount of dichloromethane and then adding hexane until the solution just turns cloudy. After 7 days at −20 °C, rod-shaped, yellow crystals are isolated. The compound is considerably more air- and moisture-sensitive than "open ruthenocene" but may be handled in the atmosphere for short periods of time. The salt is insoluble in all hydrocarbon and ether solvents, but it dissolves readily in dichloromethane and nitromethane. Anal. Calcd for $C_{14}H_{23}BF_4Ru$: C, 44.34; H, 6.11. Found: C, 44.17; H, 6.35. ^1H NMR (CD_3NO_2, 60 °C): δ 5.62 (s, 2 H), 2.11 (s, 12 H), 1.36 (br s, 9 H). ^1H NMR (CD_2Cl_2, ambient temperature): δ 5.59 (s, 2 H), 2.08 (s, 12 H). ^1H NMR (CD_2Cl_2, −50 °C): δ 5.54 (s, 2 H), 3.16 (s, 4 H), 2.01 (s, 12 H), 1.16 (s, 4 H), −5.84 (s, 1 H). ^1H NMR (CD_2Cl_2, 500 MHz, −100 °C): δ 2.98 (s, 2 H), 2.00 (s, 6 H), 1.92 (s, 6 H), 1.22 (s, 2 H), −5.84 (quintet, 1 H, J = 7.7 Hz). ^1H NMR (CD_2Cl_2, 500 MHz, −110 °C): δ 6.02 (s, 1 H), 4.96 (s, 1 H), 4.26 (s, 1 H), 2.96 (s, 2 H), 2.21 (s, 2 H), 2.00 (s, 6 H), 1.92 (s, 6 H), 1.22 (s, 1 H), 1.05 (s, 1 H), −0.17 (s, 1 H), −5.84 (s, 1 H). ^{13}C NMR (CD_2Cl_2, −56 °C): δ 97.5 (d, J = 158 Hz), 25.1 (q, J = 128 Hz). ^{13}C NMR (CD_2Cl_2, −90 °C): 112.6 (s), 97.5 (br), 61.9 (t, J = 159 Hz), 26.3 (q, J = 129 Hz), 25.0 (q, J = 129 Hz). IR (Nujol mull): 3120 (vw), 3070 (w), 1511 (w), 1494 (m), 1282 (m), 1261 (m), 1215 (vw), 1178 (mw), 1098 (vs), 1061 (vs), 1045 (sh), 973 (w), 942 (w), 863 (w), 828 (sh), 808 (m), 722 (m) cm^{-1}.

Hydridobis(2,4-dimethylpentadienyl)osmium Tetrafluoroborate, $HOs(2,4\text{-}C_7H_{11})_2^+BF_4^-$. This compound may be prepared from $Os(2,4\text{-}C_7H_{11})_2$[8] and isolated in essentially quantitative yields by following the procedure for the analogous ruthenium compound. Anal. Calcd for $C_{14}H_{23}BF_4Os$: C, 35.90; H, 4.95. Found: C, 35.87; H, 5.05. ^1H NMR (CD_2Cl_2, ambient temperature): δ 6.37 (s, 2 H), 2.17 (s, 12 H). ^1H NMR (CD_2Cl_2, 34.5 °C): δ 6.37 (s, 2 H), 2.17 (s, 12 H), 1.24 (br, 9 H). ^1H NMR (CD_2Cl_2, −96 °C): δ 6.35 (s, 2 H), 3.41 (s, 4 H), 1.97 (s, 12 H), 1.90 (s, 4 H), −7.69 (s, 1 H). ^{13}C NMR (CD_2Cl_2, −91.5 °C): δ 104.9 (s), 95.2 (d, J = 166 Hz), 42.6 (t, J = 161 Hz), 23.5 (q, J = 128 Hz). IR (Nujol mull): 3025 (w), 3018 (vw), 1518 (mw), 1506 (m), 1367 (ms), 1289 (m), 1262 (m), 1210 (w), 1100 (ms), 1060 (vs), 1041 (s), 1008 (m), 877 (w), 860 (w), 758 (m), 721 (m) cm^{-1}.

Carbonyl(η^4-dimethylpentadiene)(η^5-2,4-dimethylpentadienyl)ruthenium(II) Tetrafluoroborate, $[Ru(\eta^5\text{-}2,4\text{-}C_7H_{11})(\eta^4\text{-}2,4\text{-}C_7H_{12})CO]^+BF_4^-$. Freshly prepared $[Ru(2,4\text{-}C_7H_{11})(2,4\text{-}C_7H_{12})]^+BF_4^-$ (1.03 g, 2.72 mmol) was dissolved in 20 mL of CH_2Cl_2 and stirred for 6–8 h between 0 and 18 °C under an atmosphere of carbon monoxide. The resulting solution appeared as a slightly lighter shade of yellow compared to the original hydride solution. The volume of this solution was reduced in vacuo until crystallization began to occur. Next, 3–4 mL of ether was added in order to induce crystallization of the product, after which the mixture was cooled to −20 °C overnight. After draining for 30 min, the supernatant was removed, leaving behind 1.00 g (90% yield) of the yellow crystalline monocarbonyl product. X-ray-quality crystals (mp 140–142 °C dec) were formed by slowly cooling a saturated ethanol solution of the compound to −20 °C. Anal. Calcd for $C_{15}H_{23}BF_4ORu$: C, 44.24; H, 5.69. Found: C, 44.35; H, 5.79. ^1H NMR (CD_2Cl_2, $CDHCl_2$ reference δ 5.32, ambient temperature): δ 6.18 (1 H, s) 5.22 (1 H, s), 3.67 (1 H, d of d, J = 3.4, 1.3 Hz), 3.10 (1 H, d of d, J = 3.9, 0.7 Hz), 2.54 (1 H, d, J = 3.5 Hz), 2.41 (1 H, d of d, J = 3.5, 0.6 Hz), 2.36 (3 H, s), 2.26 (3 H, s), 1.99 (3 H, s), 1.69 (3 H, s), 1.56 (1 H, d, J = 3.4 Hz), 1.49 (1 H, d, J = 3.9 Hz), 1.46 (3 H, s). ^{13}C NMR (CD_2Cl_2, solvent reference δ 53.8, ambient temperature): δ 206.8 (s), 117.4 (s), 116.9 (s), 110.7 (q, J = 5.4 Hz), 103.2 (m (possible quintet), J = 4.3 Hz), 102.4 (d, J = 166 Hz), 91.5 (d, J = 166 Hz), 58.8 (t, J = 162 Hz), 53.2 (t, J = 162 Hz), 50.2 (t, J = 162 Hz), 29.1 (q of t, J = 128, 4.7 Hz), 25.3 (q, J = 128 Hz), 25.0 (q, J = 128 Hz), 23.6 (q, J = 129 Hz), 22.3 (q, J = 128 Hz). IR (Nujol mull): 3125 (sh), 3108 (w), 3062 (w), 2735 (mw), 2130 (sh), 2115 (m), 2025 (s), 1980 (sh), 1575 (mw), 1514 (m), 1330 (mw), 1285 (sh), 1278 (m), 1262 (mw), 1202 (mw), 1157 (sh), 1120–950 (vs), 903 (m), 862 (m), 837 (m), 807 (m), 762 (w), 720 (m) cm^{-1}. IR (CH_2Cl_2 solution): ν_{CO} = 2046 cm^{-1}. Mass spectrum (FAB, *m*-nitrobenzyl alcohol matrix): *m/e* (relative intensity) 147 (36), 191 (17), 193 (15), 195 (26), 196 (15), 207 (14), 287 (65), 289 (33), 290 (47), 291 (64), 292 (64), 293 (100), 295 (28), 318 (35), 319 (32), 320 (46), 321 (62), 323 (39).

Tricarbonyl(2,4-dimethylpentadienyl)ruthenium(II) Tetrafluoroborate, $[Ru(2,4\text{-}C_7H_{11})(CO)_3]^+BF_4^-$. A solution of

---

(3) (a) Ernst, R. D. *Chem. Rev.* **1988**, *88*, 1255. (b) Powell, P. In *Advances in Organometallic Chemistry*; West, R., Stone, F. G. A., Eds,; Academic Press: New York, 1986; Vol. 26, p 125. (c) Kreiter, C. G. In ref 3b, p 297. (d) Yasuda, H.; Nakamura, A. *J. Organomet. Chem.* **1985**, *285*, 15. (e) Bleeke, J. R.; Rauscher, D. J. *Organometallics* **1988**, *7*, 2328. (f) Lee, G.-H.; Peng, S.-M.; Lush, S.-F.; Mu, D.; Liu, R.-S. *Organometallics* **1988**, *7*, 1155.

(4) (a) Melendez, E.; Arif, A. M.; Ziegler, M. L.; Ernst, R. D. *Angew. Chem., Int. Ed. Engl.* **1988**, *27*, 1099. (b) Kralik, M. S.; Hutchinson, J. P.; Ernst, R. D. *J. Am. Chem. Soc.* **1985**, *107*, 8296.

(5) (a) Crabtree, R. H.; Dion, R. P. *J. Chem. Soc., Chem. Commun.* **1984**, 1260. (b) Werner, R; Werner, H. *Chem. Ber.* **1984**, *117*, 161. (c) Derome, A. E.; Green, M. L. H.; O'Hare, D. *J. Chem. Soc., Dalton Trans.* **1986**, 343. (d) Bleeke, J. R.; Moore, D. A. *Inorg. Chem.* **1986**, *25*, 3522. (e) Bleeke, J. R.; Kotyk, J. J.; Moore, D. A.; Rauscher, D. J. *J. Am. Chem. Soc.* **1987**, *109*, 417.

(6) Ether and hydrocarbon solvents were distilled under nitrogen from the benzophenone radical anion and/or dianion. CH_2Cl_2 was distilled under nitrogen from P_4O_{10}, while methanol, ethanol, and nitromethane were stored for at least several days over molecular sieves and then subjected to several freeze–thaw degassing cycles.

(7) Stahl, L.; Ernst, R. D. *Organometallics* **1983**, *2*, 1229.

(8) Stahl, L.; Ma, H.; Ernst, R. D.; Hyla-Kryspin, I.; Gleiter, R.; Ziegler, M. L. *J. Organomet. Chem.* **1987**, *326*, 257.

$[Ru(2,4\text{-}C_7H_{11})(2,4\text{-}C_7H_{12})]^+BF_4^-$ (0.52 g, 1.38 mmol) in 20 mL of ethanol was stirred at 70 °C for 1–2 h under a carbon monoxide atmosphere, resulting in a solution that appeared almost colorless. The reaction mixture was then evaporated to dryness in vacuo, the residue extracted into 15 mL of CH_2Cl_2, and the extract filtered, after which the volume was reduced in vacuo until crystallization began to occur. The addition of 5 mL of Et_2O precipitated much of the product, and additional cooling to −20 °C overnight followed by draining for 2 h resulted in the isolation of 0.41 g (80%) of the colorless crystalline product (decomposition, 211–214 °C). Anal. Calcd for $C_{10}H_{11}BF_4O_3Ru$: C, 32.72; H, 3.02. Found: C, 32.72; H, 3.04. ^1H NMR (CD_3NO_2, CD_2HNO_2 reference δ 4.33, ambient temperature): δ 6.71 (1 H, br, s), 3.68 (2 H, d of d, J = 3.9, 1.5 Hz), 2.52 (6 H, s), 2.20 (2 H, d of d, J = 3.9, 0.6 Hz). ^{13}C NMR (CD_3NO_2, solvent reference δ 62.8, ambient temperature): δ 192.4 (1 C, s), 187.1 (2 C, s), 131.0 (s), 98.0 (d, J = 174 Hz), 60.3 (t, J = 162 Hz), 27.3 (q, J = 130 Hz). IR (Nujol mull): 3130 (vw), 3100 (vw), 3060 (vw), 2720 (vw), 2125 (sh), 2070 (s), 2040 (s), 2000 (s), 1985 (sh), 1730 (w), 1518 (w), 1280 (m), 1265 (sh), 1098 (ms), 1040 (s), 975 (m), 930 (w), 862 (m), 722 (m) cm^{-1}. IR (CH_2Cl_2 solution): ν_{CO} = 2130, 2084 (sh), 2076 cml^{-1}. Mass spectrum (FAB, *m*-nitrobenzyl alcohol matrix): *m/e* (relative intensity) 250 (12), 251 (12), 253 (22), 280 (25), 281 (100), 283 (28).

Carbonylbis(triethylphosphine)(2,4-dimethylpentadienyl)ruthenium(II) Tetrafluoroborate, $[Ru(2,4\text{-}C_7H_{11})(P(C_2H_5)_3)_2CO]^+BF_4^-$. A solution of $[Ru(2,4\text{-}C_7H_{11})(2,4\text{-}C_7H_{12})CO]^+BF_4^-$ (0.56 g, 1.38 mmol) in 20 mL of ethanol was stirred at 0 °C while triethylphosphine (1.00 mL, 8.46 mmol) was added via syringe. The solution was stirred for 15 min and then refluxed for 1 h before the solvent was removed in vacuo, leaving behind a pale yellow oily residue. The residue was washed (lightly) with ether and then dissolved in 5 mL of ethanol. Addition of an equal volume of Et_2O initiated crystallization of the product, while subsequent cooling to −20 °C overnight allowed more complete crystallization. The supernatant was removed, and the product (0.39 g, 49% based on 1:1 complexation with EtOH) in the form of colorless bar-shaped prisms (mp 149–150 °C) was drained well and dried in vacuo for 30 s. The product was recrystallized from EtOH/Et_2O and then dried under a stream of nitrogen after removal of the supernatant. A single crystal suitable for X-ray diffraction was cleaved from one of the bar-shaped prisms and sealed in a 0.5-mm glass capillary. NMR spectra were also recorded on a sample prepared from the same batch of crystals dissolved in CD_3NO_2. The remaining crystals were held under dynamic vacuum for at least 4 h before being sealed under vacuum in glass and set for C, H analysis. Anal. Calcd for $C_{20}H_{41}BF_4OP_2Ru$: C, 43.89; H, 7.55. Found: C, 43.59; H, 7.95. ^1H NMR (CD_3NO_2, CD_2HNO_2 reference δ 4.33, ambient temperature): δ 6.00 (1 H, s), 3.57* (2 H, m (pseudoquintet or d of q), J = 7 Hz), 3.15* (1 H, s (broad)), 3.00 (1 H, s (broad)), 2.30 (3 H, s), 2.27 (3 H, s), 2.11–2.23 (7 H, m), 1.96–2.11 (3 H, m), 1.66–1.80 (3 H, m), 1.10–1.27 (22 H, m), 0.86 (1 H, s (broad)). ^{13}C NMR (CD_3NO_2, solvent reference δ 62.8, ambient temperature): δ 201.4 (CO, d of d, J(PC) = 17, 11 Hz), 128.6 (s), 117.3 (s), 93.2 (d of d of d, J(CH) = 166, J(PC) = 8, 1 Hz), 66.7* (t, J = 140 Hz), 57.8 (t of d, J(CH) = 160, J(PC) = 20 Hz), 54.2 (t, J(CH) = 159 Hz), 27.3 (q, J = 128 Hz), 27.0 (q, J = 129 Hz), 23.3 (PCH_2, t of d, J(CH) = 129, J(PC) = 30 Hz), 20.6 (PCH_2, t of d, J(CH) = 129, J(PC) = 26 Hz), 15.7* (CH_3, q, J(CH) = 125 Hz), 9.7 (CH_3 from PEt_3, q of q, J(CH) = 128, 5, J(PC) = 5 Hz), 8.2 (CH_3 from PEt_3, q of m, J(CH) = 128, J(PC) = 4 Hz). The asterisks denote resonances resulting from ethanol. The methyl proton signals for ethanol in the ^1H NMR spectrum are presumably hidden in the multiplet between 1.10 and 1.27 ppm. $^{31}P\{^1H\}$ NMR (CD_3NO_2, H_3PO_4 reference δ 0.0, ambient temperature): δ 30.0 (d, J(PP) = 22 Hz), 26.6 (d, J(PP) = 22 Hz). IR (Nujol mull): 3900 (w), 3550 (vw), 3115 (w), 3095 (w), 3055 (m), 2727 (w), 2670 (sh), 2460 (w), 1960 (s), 1915 (sh), 1890 (sh), 1960 (s), 1915 (sh), 1890 (sh), 1570 (w), 1280 (ms), 1269 (ms), 1243 (sh), 1202 (vw), 1100–980 (s), 930 (m), 860 (m), 799 (mw), 753 (s), 735 (s), 718 (s), 704 (sh), 660 (mw), 639 (m), 607 (m) cm^{-1}. IR (CH_2Cl_2 solution): ν_{CO} = 1974 cm^{-1}. Mass spectrum (FAB, *m*-nitrobenzyl alcohol matrix): *m/e* (relative intensity) 313 (11), 340 (10), 341 (11), 342 (30), 343 (46), 345 (13), 458 (37), 459 (36), 460 (54), 461 (100), 463 (52).

Tris(trimethylphosphine)(2,4-dimethylpentadienyl)ruthenium(II) Tetrafluoroborate, $[Ru(2,4\text{-}C_7H_{11})(P(CH_3)_3)_3]^+BF_4^-$. Freshly prepared $[Ru(2,4\text{-}C_7H_{11})(2,4\text{-}C_7H_{12})]^+BF_4^-$ (0.441 g, 1.16 mmol) was dissolved in 15 mL of CH_2Cl_2; then with stirring, 5 equiv of trimethylphosphine (0.55 mL) was added via syringe and stirring was continued overnight. The volatile components were then removed in vacuo, after which the remaining residue was extracted into CH_3OH and the extract filtered through Celite. The volume was reduced in vacuo until crystallization began (ca. 10 mL of solution), after which cooling to −20 °C led to the formation of light yellow rectangular bar-shaped crystals (0.27 g, 46%; decomposition, 215 °C), which were drained and the supernatant was removed before the crystals were dried in vacuo. Another batch of crystals (0.29 g, 48%) was obtained by further reducing the volume of the supernatant and cooling again to −20 °C. Anal. Calcd for $C_{16}H_{38}BF_4P_3Ru$: C, 37.59; H, 7.66. Found: C, 37.70; H, 7.66. ^1H NMR (CD_2Cl_2, $CDHCl_2$ reference δ 5.32, ambient temperature): δ 5.51 (1 H, s), 2.32 (2 H, m (apparent seven-line pattern), J = 1.8 Hz), 2.18 (6 H, q, J = 1.3 Hz), 1.65 (9 H, br), 1.39 (18 H, br), 0.69 (2 H, s). ^{13}C NMR (CD_2Cl_2, solvent reference δ 53.8, 2 °C): δ 118.5 (s), 88.8 (d of d, J(CH) = 163, J(CP) = 7 Hz), 52.1 (CH_2, t of m, J(CH) = 156, J(CP) = ca. 2–4 Hz), 26.0 (CH_3, q, J(CH) = 128 Hz), 24.1 (PMe_3, q of d, J(CH) = 128 Hz, J(CP) = 30 Hz), 22.3 (PMe_3, q of t, J(CH) = 128 Hz, J(CP) = 15 Hz). $^{31}P\{^1H\}$ NMR (CD_3NO_2, H_3PO_4 reference δ 0.0, 2 °C): δ −0.5 (1 P, t, J(PP) = 28 Hz), −2.9 (2 P, d, J(PP) = 28 Hz). IR (Nujol mull): 3120 (vw), 3060 (vw), 1515 (sh), 1500 (mw), 1305 (m), 1291 (m), 1284 (m), 1093 (s), 1047 (vs), 1034 (sh), 960 (sh), 940 (vs), 925 (sh), 855 (m), 719 (s), 678 (sh), 669 (m) cm^{-1}. Mass spectrum (FAB, *m*-nitrobenzyl alcohol matrix): *m/e* (relative intensity) 206 (10), 207 (10), 209 (14), 211 (11), 219 (12), 221 (10), 222 (12), 224 (14), 236 (11), 238 (15), 239 (12), 241 (11), 251 (34), 252 (46), 253 (15), 266 (12), 267 (14), 268 (12), 269 (47), 270 (35), 271 (36), 272 (12), 273 (10), 345 (15), 346 (42), 347 (67), 348 (67), 349 (100), 350 (11), 351 (50), 424 (8), 425 (14), 427 (10).

Dicarbonyl(triethylphosphine)(2,4-dimethylpentadienyl)ruthenium(II) Tetrafluoroborate, $[Ru(2,4\text{-}C_7H_{11})(P(C_2H_5)_3)(CO)_2]^+BF_4^-$. Freshly prepared $[Ru(2,4\text{-}C_7H_{11})(2,4\text{-}C_7H_{12})]^+BF_4^-$ (0.425 g, 1.12 mmol) was stirred in EtOH at −78 °C whereupon 1 equiv of triethylphosphine (0.132 g, 0.165 mL) in 3 mL of CH_2Cl_2 was added dropwise. The solution was stirred while being warmed to −40 °C over $^1/_2$ h, after which time carbon monoxide was slowly admitted into the flask. The solution was then warmed slowly while being stirred under an atmosphere of carbon monoxide. The volume of the resulting pale yellow solution was reduced in vacuo until crystallization began (ca. 5 mL), at which point 3–4 mL of Et_2O was added, forcing much of the product out of solution. After the solution was cooled for 3–4 h to −20 °C, the supernatant was removed and the off-white microcrystalline product (0.250 g, 49%) was dried in vacuo. Crystals (mp 193–197 °C) suitable for X-ray diffraction were grown from a saturated EtOH solution by slow cooling to 0 °C. Anal. Calcd for $C_{15}H_{26}BF_4O_2PRu$: C, 39.40; H, 5.73. Found: C, 39.42; H, 5.73. ^1H NMR (CD_2Cl_2, $CDHCl_2$ reference δ 5.32, ambient temperature): δ 6.31 (1 H, s), 3.13 (2 H, m, J = 2.5 Hz from H(n), smaller coupling from ^{31}P and H(3) <1.6 Hz), 2.38 (3 H, s), 2.22 (6 H, d of q, J(PH) = 9.2 Hz, J(HH) = 7.6 Hz), 1.56 (2 H, m (apparent triplet), J = 2.5 Hz from H(x) and ^{31}P), 1.22 (9 H, d of t, J(PH) = 17.6, J(HH) = 7.6 Hz). ^{13}C NMR (CD_2Cl_2, solvent reference δ 52.8, ambient temperature): δ 192.2 (CO, d, J(CP) = 10.8 Hz), 126.3 (s), 95.2 (d of d, J(CH) = 172, J(CP) = 7.2 Hz), 58.3 (t, J = 159 Hz), 27.5 (q, J = 129 Hz), 22.2 (PCH_2, t of d, J(CH) = 129, J(CP) = 32 Hz), 7.98 (CH_3 from PEt_3, q of t of d, J(CH) = 129, 5, J(CP) = 4 Hz). $^{31}P\{^1H\}$ NMR (CD_3NO_2, H_3PO_4 reference δ 0.00, ambient temperature): δ 34.4 (s). IR (Nujol mull): 3120 (m), 3065 (w), 2065 (vs), 2015 (vs), 1953 (s), 1511 (w), 1490 (w), 1398 (m), 1280 (m), 1256 (m), 1238 (sh), 1205 (vw), 1110–1000 (vs), 954 (sh), 868 (ms), 811 (w), 794 (w), 768 (ms), 757 (m), 721 (s), 714 (s), 628 (mw) cm^{-1}. IR (CH_2Cl_2 solution): ν_{CO} = 2063, 2015 cm^{-1}. Mass spectrum (FAB, *m*-nitrobenzyl alcohol matrix): *m/e* (relative intensity) 252 (10), 311 (12), 312 (11), 313 (37), 315 (10), 340 (14), 341 (36), 342 (36), 343 (63), 345 (34), 368 (41), 369 (48), 370 (60), 371 (100), 372 (10), 373 (58).

Reaction of $Ru(2,4\text{-}C_7H_{11})(2,4\text{-}C_7H_{12})(CO)^+$ with PMe_3. Crystalline $[Ru(2,4\text{-}C_7H_{11})(2,4\text{-}C_7H_{12})CO]^+BF_4^-$ (0.34 g, 0.83 mmol) was added to a solution of trimethylphosphine (0.41 g, 5.4 mmol) in 10 mL of methanol at −78 °C. Initially, the mixture appeared

Table I. Summary of the Diffraction Studies for $Os(C_5H_5)(2,4\text{-}C_7H_{11})$ (I), $Ru(2,4\text{-}C_7H_{11})(\eta^4\text{-}2,4\text{-}C_7H_{12})(CO)^+BF_4^-$ (II), $Ru(2,4\text{-}C_7H_{11})(CO)_2(PEt_3)^+BF_4^-$ (III), and $Ru(2,4\text{-}C_7H_{11})(CO)(PEt_3)_2{}^+BF_4^-$ (IV)

	I	II	III	IV
formula	$OsC_{12}H_{16}$	$RuC_{15}H_{23}OBF_4$	$RuC_{15}H_{26}O_2PBF_4$	$RuC_{22}H_{47}O_2P_2BF_4$
mol wt	350.5	407.2	457.2	593.5
space group	*Pnma*	$P2_1/n$	$P2_1/m$	$P2_1/n$
lattice constants				
a, Å	5.900 (2)	8.436 (6)	8.863 (2)	10.809 (3)
b, Å	13.089 (7)	13.818 (4)	12.246 (2)	27.134 (7)
c, Å	13.503 (6)	15.199 (9)	9.801 (2)	10.879 (3)
β, deg	90	104.72 (5)	112.98 (2)	115.40 (2)
V, Å^3	1042.8	1713.6	979.35	2882.3
Z	4	4	2	4
d(calc), g cm^{-3}	1.72	1.58	1.55	1.37
γ, Å	0.71073	0.71073	0.71073	0.71073
temp, °C	20	20	20	20
cryst shape; size, mm	parallelpiped; 0.20 × 0.25 × 0.40	irregular; 0.26 × 0.50 × 0.54	plate; 0.12 × 0.31 × 0.34	parallelpiped; 0.19 × 0.27 × 0.34
linear abs coeff, cm^{-1}	121.98	9.32	9.04	6.80
scan type	θ–2θ	Ω	Ω	Ω
scan speed, deg min^{-1}	3–29	2–4	2–4	2–4
abs treatment	ψ scan (0.412–1.000)	ψ scan (0.85–1.00)	ψ scan (0.85–1.00)	ψ scan (0.84–1.00)
scan range, deg	1.4	1.05	1.05	1.05
2θ limits, deg	3–60	3–70	2.5–65	3–46
min *hkl*	000	0,–22,–25	0,0,–15	0,0,–12
max *hkl*	9,19,19	14,0,25	13,19,15	12,30,12
no. of unique data with $I > 2.5\sigma(I)$	1176	2337	2337	1578
R(*F*)	0.043	0.053	0.037	0.067
$R_w(F)$	0.044	0.046	0.032	0.054
GOF	4.0	2.2	2.8	2.1
max diff Fourier peak, e Å^{-3}	1.88	0.72	0.55	0.60

as a yellow slurry that, after it was stirred for 3 h while being warmed at room temperature, turned a very pale yellow color. The volatile components were then removed in vacuo, and the remaining solid was washed twice with ether. After it was dried, the product was isolated analytically pure as a pale yellow microcrystalline powder (0.33 g, 81%). The product was recrystallized as thick yellow plates (mp 145–146 °C) from a concentrated solution in CH_2Cl_2/Et_2O cooled to –20 °C. Anal. Calcd for $C_{18}H_{32}BF_4OPRu$: C, 44.73; H, 6.67. Found: C, 44.76; H, 7.00. ^{1}H NMR (CD_3NO_2, CD_2HNO_2 reference δ 4.33, ambient temperature): δ 5.04 (1 H, s), 3.38 (1 H, t, *J* = 1.5 Hz), 3.29 (1 H, d, *J* = 1.4 Hz), 2.62 (1 H, d, *J*(HP) = 13 Hz), 2.38 (1 H, t, *J* = 1.5 Hz), 2.24 (1 H, d, *J* = 1.5 Hz), 2.12 (3 H, s), 2.09 (3 H, s), 2.06 (3 H, s), 1.86 (9 H, d, *J*(PH) = 13 Hz), 1.33 (3 H, d, *J*(HP) = 17 Hz), 0.95 (1 H (partially hidden from view by overlap of the left side of the doublet at δ 0.92)), 0.92 (3 H, d, *J*(HP) = 18 Hz), 0.87 (1 H, d, *J* = 2 Hz). ^{13}C NMR (CD_3NO_2, solvent reference δ 62.8, ambient temperature): δ 215.0 (s), 112.7 (s), 111.8 (s), 103.2 (d, *J*(CH) = 170 Hz), 96.5 (d, *J*(CP) = 4 Hz), 62.1 (d of d, *J*(CH) = 170, *J*(CP) = 4 Hz), 52.9 (t of d, *J*(CH) = 160 Hz, *J*(CP) = 4 Hz), 49.8 (t, *J*(CH) = 160 Hz), 46.1 (t, *J*(CH) = 160 Hz), 38.6 (d of t, *J*(CP) = 66, *J*(CH) = 1.5 Hz), 30.4 (q, *J*(CH) = 130 Hz), 25.6 (q of d, *J*(CH) = 130, *J*(CP) = 5 Hz), 25.4 (q, *J*(CH) = 129 Hz), 24.9 (q, *J*(CH) = 129 Hz), 18.3 (q of d, *J*(CH) = 129, *J*(CP) = 5.6 Hz), 6.5 (q of d, *J*(CH) = 129, *J*(CP) = 83 Hz). ^{31}P{^{1}H} NMR (CD_3NO_2, H_3PO_4 reference δ 0.0, ambient temperature): δ 39.1 (s). IR (Nujol mull): 3840 (w), 3095 (w), 3085 (w), 2730 (vw), 2000 (sh), 1933 (s), 1889 (sh), 1820 (sh), 1570 (w), 1503 (mw), 1389 (m), 1350 (mw), 1325 (mw), 1308 (m), 1288 (mw), 1261 (vw), 1142 (sh), 1105 (sh), 1050 (s), 1035–1020 (vs), 988 (sh), 970 (sh), 961 (s), 924 (sh), 912 (sh), 898 (sh), 875 (sh), 861 (m), 809 (vw), 778 (sh), 767 (m), 720 (w), 704 (mw), 631 (w) cm^{-1}. IR (CH_2Cl_2 solution): ν_{CO} = 1960 cm^{-1}. Mass spectrum (FAB, *m*-nitrobenzyl alcohol matrix): *m/e* (relative intensity) 290 (63), 291 (50), 292.9 (61), 293 (63), 295 (20), 315 (12), 318 (22), 319 (66), 320 (66), 321 (100), 323 (78), 396 (16), 397 (19), 399 (13).

X-ray Diffraction Studies. Single crystals of the compounds investigated were grown as described in the foregoing experimental descriptions. Pertinent data collection and structural quality indicators are summarized in Table I. Data for the osmium complex were collected on a Syntex R3 diffractometer, while the other data sets were collected on a Siemens-Stoe AED-II diffractometer. The SHELXTL program package was employed for structure solutions. All structures were solved via Patterson syntheses, after which the remaining atoms were located via successive Fourier maps and least-squares refinements. In the refinements the function minimized was $\sum w(|F_o| - |F_c|)$, for which $w = 1/\sigma^2(F)$. Hydrogen atoms were located from difference Fourier maps and generally placed in idealized locations at a distance of 0.96 Å from the attached carbon atoms.[9] In several of the structures, the BF_4^- groups was subjected to disorder, and additional fluorine atom locations, with partial occupancy factors, had to be included.

Synthetic Results and Discussion

Analogous to results for $Ru(C_5H_5)(2,4\text{-}C_7H_{11})$ (C_7H_{11} = dimethylpentadienyl),[10] $Ru(C_5Me_5)(\eta^5\text{-}C_8H_{11})$[11] ($C_8H_{11}$ = cyclooctadienyl), $Ru(\eta^5\text{-}C_8H_{11})_2$,[11] and a number of other open (η^5-dienyl)metal complexes,[5] both $Ru(2,4\text{-}C_7H_{11})_2$ and $Os(2,4\text{-}C_7H_{11})_2$ may readily be protonated by HBF_4, yielding white, air-sensitive precipitates (eq 1). At first

$$M(2,4\text{-}C_7H_{11})_2 + HBF_4 \xrightarrow{\text{ether}} \text{“}HM(2,4\text{-}C_7H_{11})_2{}^{+}\text{”} \qquad (1)$$

glance, variable-temperature ^{1}H NMR spectroscopy seemed to be in accord with protonation at the metal centers, as had first been proposed,[10,11] in that well-defined signals were found at –5.84 (quintet, M = Ru) and –7.69 (singlet, M = Os) ppm, although at higher temperatures exchange between the "hydride" ligand and the hydrogen atoms of the terminal CH_2 groups occurred, similar to the case for $Ru(C_5H_5)(\eta^6\text{-}2,4\text{-}C_7H_{12})^+$ ("$HRu(C_5H_5)(2,4\text{-}C_7H_{11})^+$") and several other (pentadienyl)metal compounds.[5,10,11] Thus, at 40 °C only three resonances were

---

(9) For $Os(C_5H_5)(2,4\text{-}C_7H_{11})$, only the hydrogen atoms on the open ligand could be located. For the methyl group, these were idealized to a tetrahedral geometry having *d*(C–H) = 0.96 Å, while the other hydrogen atom locations were simply taken from the differences Fourier map.

(10) Gleiter, R.; Hyla-Kryspin, I.; Ziegler, M. L.; Sergeson, G.; Green, J. C.; Stahl, L.; Ernst, R. D. *Organometallics* **1989**, *8*, 298.

(11) (a) Bouachir, F.; Chaudret, B.; Tkatchenko, I. *J. Chem. Soc., Chem. Commun.* **1986**, 94. (b) Cox, D. N.; Roulet, R. *J. Chem. Soc., Chem. Commun.* **1988**, 951; **1989**, 175.

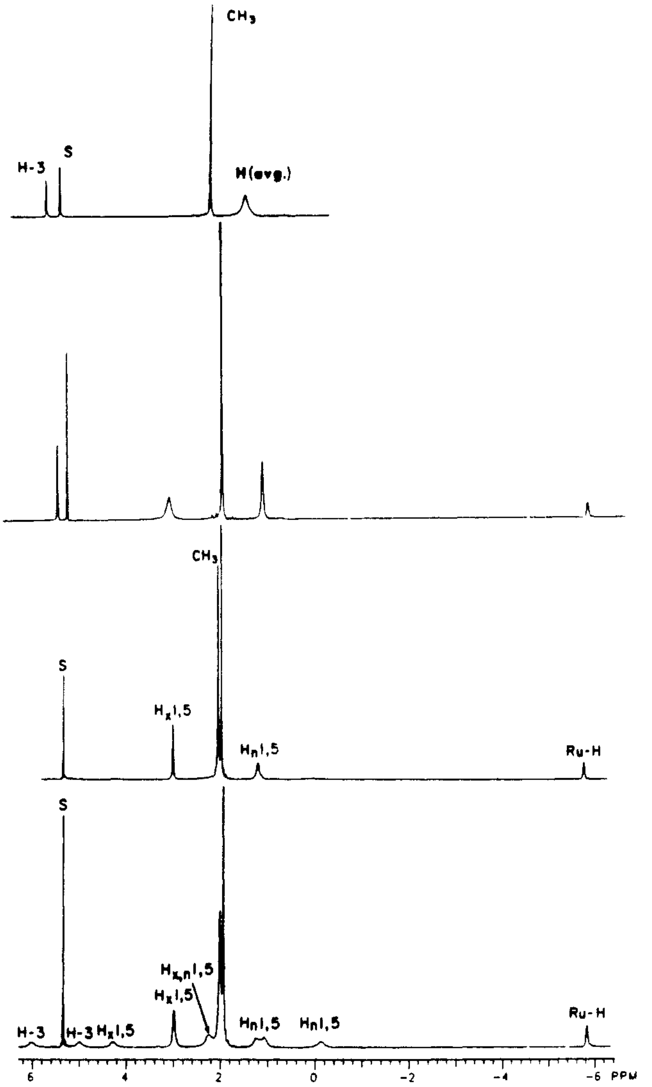

Figure 1. ^{1}H NMR spectra of "$HRu(2,4\text{-}C_7H_{11})_2{}^+$" at 40 °C (top, 300 MHz), -50 °C (second from top, 300 MHz), -100 °C (second from bottom, 500 MHz), and -110 °C (bottom, 500 MHz). Subscripts n and x designate endo and exo, respectively. Some of the methyl resonances have been truncated for clarity.

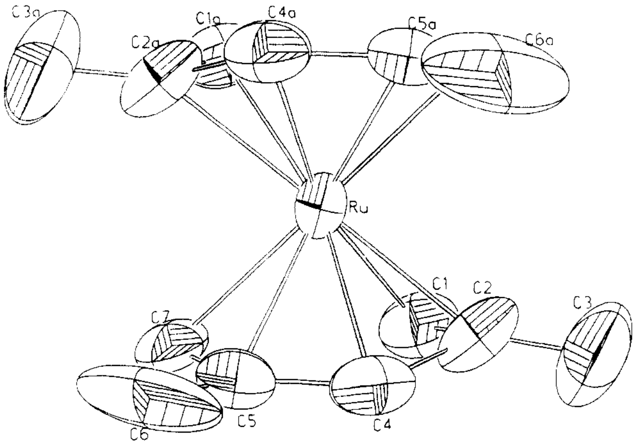

Figure 2. General structure of "$HRu(2,4\text{-}C_7H_{11})_2{}^+$".

observed (5.62, 2.11, and 1.36 ppm), which were integrated in a 2:12:9 ratio, corresponding to the central hydrogen atoms (on the C3's), the methyl groups, and the average hydride and CH_2 resonances (Figure 1). When the compound is cooled, however, these resonances broaden and ultimately decoalesce. By -50 °C, a well-defined 2:4:12:4:1 pattern of resonances is observed, attributable to the H3, H1,5 exo, CH_3, H1,5 endo, and hydride sites, consistent either with a symmetric, syn-eclipsed structural pattern (I) or with an unsymmetric conformation undergoing rapid ligand oscillation on the NMR time scale. In fact, further cooling leads to additional decoalescence of the five-line pattern, indicating that the actual ground state possesses no symmetry. Thus, all hydrogen atoms bound to sp^2-hybridized carbon atoms become inequivalent, as can be seen in Figure 1. Two factors contribute to these extra complications. A recent NMR spectroscopic study (145-300 K) on "$HRu(2,4\text{-}C_7H_{11})_2{}^+$" (and "$HRu(C_5H_5)(2,4\text{-}C_7H_{11})^+$") has revealed that the "hydride" ligand actually is "agostic", bridging a terminal CH_2 group and the ruthenium atom.[11] In addition, however, a structural determination of "$HRu(2,4\text{-}C_7H_{11})_2{}^+$" has revealed that a nearly gauche-eclipsed conformation is adopted (Figure 2), as in $Ru(2,4\text{-}C_7H_{11})_2$ (II), although the structure apparently suffers from a 4-fold disorder that renders all terminal carbon atoms essentially equivalent.[12] From the above results, it is clear that at least four exchange processes take place in solution, including both inter- and intraligand transfer of the "hydride" ligand from one "CH_2" (agostic CH_3) group to another CH_2, a rotation of the agostic CH_3 group, and oscillation of the two pentadienyl ligands through a symmetric, presumably syn-eclipsed, conformation. Barriers for the first three processes have been estimated by line-shape analysis, but the unsymmetric pentadienyl ligand orientation was not taken into account[11] and perhaps is responsible for the observation of a higher barrier to 1,5-intraligand hydrogen atom transfer relative to 1,1′-transfer, both of which could involve a hydride intermediate. Notably, while the barrier to ligand oscillation for $Ru(2,4\text{-}C_7H_{11})_2$ is 9.7 ± 0.1 kcal/

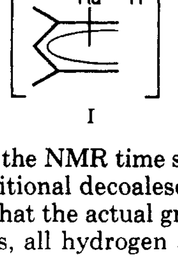

I

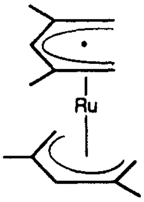

II

---

[12] (a) Crystals of "$HRu(2,4\text{-}C_7H_{11})_2{}^+BF_4{}^-$" are orthorhombic, space group $C222_1$, with a = 8.266 (2) Å, b = 13.819 (5) Å, c = 14.070 (4) Å, V = 1607.1 Å^3, and D(calc) = 1.56 g/cm^3. The structure was refined to values of R and R_W of 0.055 and 0.052, respectively, for 1292 reflections having $I > 2.5\sigma(I)$. The molecule was found to lie on a site having imposed C_2 symmetry, necessitating a disordered structure, in which each observed ligand likely represents an average of four images. Nonetheless, the Ru–C distances may have some value, being 2.288 (10), 2.189 (8), 2.142 (11), 2.183 (11), and 2.265 (9) Å, respectively, for atoms C1, C2, C4, C5 and C7. The longer, nearly equal, bonds involving C1 and C7 are consistent with a structure in which 25% of the time they are formally protonated, giving rise to an "agostic" (C–H)→M interaction. Thus, for comparison, in $Cr(\eta^6\text{-}2,4\text{-}C_7H_{12})(CO)_2[P(OMe)_3]$, which possesses an ordered "agostic" structure, the Cr–C(terminal) distances are 2.246 (4) and 2.399 (4) Å, the latter corresponding to the protonated carbon atom.[12b] (b) Michael, G.; Kaub, J.; Kreiter, C. G. *Angew. Chem., Int. Ed. Engl.* **1985**, *24*, 502.

mol, the barrier upon protonation decreases to no more than 9.3 ± 0.1 kcal/mol.

The behavior for "$HOs(2,4\text{-}C_7H_{11})_2^+$", however, differs somewhat. At the high-temperature exchange limit, one again sees a 2:12:9 pattern, which decoalesces on cooling to −96 °C to a 2:4:12:4:1 pattern. Further decoalescence was not observed (to −105 °C at 500 MHz), perhaps due either to the adoption of a normal hydride bonding mode in the syn-eclipsed structure[13] or to barriers for hydride exchange and ligand oscillation that are even lower than those for the ruthenium analogue. In this regard, one can note that the barrier for ligand oscillation in $Os(2,4\text{-}C_7H_{11})_2$ is 13.5 kcal/mol, notably higher than the value for $Ru(2,4\text{-}C_7H_{11})_2$. Additionally, it can be noted that, in the open metallocenes themselves, there is a noticeable twist away from the gauche-eclipsed toward the syn-eclipsed conformation as one passes from iron to osmium ($Fe(2,4\text{-}C_7H_{11})_2$,[14a] 59.7°; $Fe(2,3,4\text{-}C_8H_{12})_2$,[14b] 55.1°; $Ru(2,3,4\text{-}C_8H_{13})_2$,[7] 52.5°; $Os(2,4\text{-}C_7H_{11})_2$,[8] 48.2°).

As the NMR results reveal the presence of a fairly accessible 16-electron $Ru(\eta^5\text{-}2,4\text{-}C_7H_{11})(\eta^4\text{-}2,4\text{-}C_7H_{12})^+$ complex, it appeared that this cationic complex should readily incorporate additional two-electron-donor ligands with the formation of $Ru(\eta^5\text{-}2,4\text{-}C_7H_{11})(\eta^4\text{-}2,4\text{-}C_7H_{12})(L)^+$ complexes. In fact, exposure of $Ru(\eta^5\text{-}2,4\text{-}C_7H_{11})(\eta^6\text{-}2,4\text{-}C_7H_{12})^+$ to CO (or $P(OMe)_3$[15]) did lead to formation of the mono(ligand) adduct in high yield (eq 2; L = CO, $P(OMe)_3$). For the

$$\text{"}HRu(2,4\text{-}C_7H_{11})_2^{+}\text{"} + L \rightarrow Ru(\eta^5\text{-}2,4\text{-}C_7H_{11})(\eta^4\text{-}2,4\text{-}C_7H_{12})(L)^+ \quad (2)$$

monocarbonyl complex, a C–O stretching frequency of 2046 cm^{-1} was observed. With a neutral diene ligand now coordinated to the Ru(II) center, it appeared possible that addition of 2 equiv of another two-electron-donor ligand might lead to $Ru(2,4\text{-}C_7H_{11})(L)(L')_2^+$ species. This turned out to be the case. While the addition of 1 equiv of PMe_3 appeared to lead to a phosphonium–allyl complex (III),

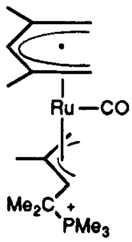

III

addition of an excess of PEt_3 under refluxing conditions did allow for isolation of pure, crystalline $Ru(2,4\text{-}C_7H_{11})(PEt_3)_2(CO)^+$ salts. Not surprisingly, $Ru(2,4\text{-}C_7H_{11})(CO)_3^+$ could be similarly prepared.

Furthermore, it also proved possible to isolate $Ru(2,4\text{-}C_7H_{11})(PEt_3)(CO)_2^+$ by a similar route, in which the order of addition was reversed. The most efficient conditions for this appear to involve the addition of 1 equiv of PEt_3 to $HRu(2,4\text{-}C_7H_{11})_2^+$ at −78 °C, after which the mixture was warmed slowly to −40 °C. Carbon monoxide was introduced into the vessel, which then was warmed slowly to room temperature, after which the desired compound could be isolated.[16] On the other hand, the use of an excess of phosphine (e.g., PMe_3) led to the clean formation of $Ru(2,4\text{-}C_7H_{11})(PMe_3)_3^+$.

As could be expected from observations on other M(dienyl)(L)$(L')_2$[17] or M(dienyl)(X)$(L)_2$[18,19] complexes, the mixed carbonyl–phosphine adducts demonstrate clear conformational preferences. While M(dienyl)$(L)_3$ complexes may be considered to be pseudooctahedral, as in IV,

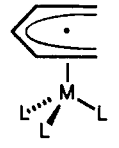

IV

a distinction between sites arises as a result of the fact that the η^5-dienyl ligand essentially occupies five sites of a hexagon, and unused metal orbital density is thus available near the sixth site, below which one ligand resides.[19] This then results in an upward tilt of the unique ligand under the open dienyl edge, as in V, rendering this site electronically and sterically different from the other two.[19] That both carbonyl and phosphine ligands prefer the unique site has been revealed through spectroscopic and diffraction studies on complexes such as $Fe(2,4\text{-}C_7H_{11})(I)(CO)_2$ and $Cr(2,4\text{-}C_7H_{11})(Cl)(dmpe)$, which are both unsymmetric, with the halide ligand located under a formally uncharged dienyl carbon atom (C2 or C4). In each case, the M–L distance involving the open edge site is shorter than that for the other site. Similar observations

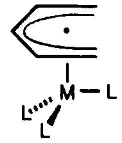

V

---

[13] It can be noted that a classical hydride structure entails a formal metal oxidation state of +4, whereas pentadienyl compounds do not favor high metal oxidation states.[3a] This may contribute to the adoption of the "agostic" structures.

[14] (a) Wilson, D. R.; Ernst, R. D.; Cymbaluk, T. H. *Organometallics* **1983**, *2*, 1220. (b) Han, J.-C.; Hutchinson, J. P.; Ernst, R. D. *J. Organomet. Chem.* **1987**, *321*, 389.

[15] Treatment of "$HRu(2,4\text{-}C_7H_{11})_2BF_4$" with 1 equiv of $P(OMe)_3$ in nitromethane at room temperature leads to the instant formation of $Ru(\eta^5\text{-}2,4\text{-}C_7H_{11})(\eta^4\text{-}2,4\text{-}C_7H_{12})[P(OMe)_3]^+BF_4^-$, while treatment with 3 equiv of $P(OMe)_3$ at 80 °C for 20 min leads to the formation of $Ru(\eta^5\text{-}2,4\text{-}C_7H_{11})[P(OMe)_3]_3^+BF_4^-$, both reactions proceeding in high yield. Spectroscopic data are quite analogous to those for the carbonyl and phosphine analogues. Data for the mono(phosphite) adduct are as follows. ^1H NMR (299.9 MHz, 18.1 °C, CD_3NO_2): δ 5.95 (s, 1 H), 4.94 (s, 1 H), 4.07 (d, 9 H, *J* = 11.5 Hz), 3.67 (d, 1 H, *J* = 4.3 Hz), 3.02 (d, 1 H, *J* = 3.9 Hz), 2.40 (d, 1 H, *J* = 2.9 Hz), 2.22 (s, 3 H), 2.19 (s, 3 H), 1.88 (s, 3 H), 1.81 (d of d, 1 H, *J* = 3.2, 13.7 Hz), 1.46 (s, 3 H), 1.06 (d, 3 H, *J* = 2.8 Hz), 0.95 (d of d, 1 H, *J* = 3.4, 6.9 Hz), 0.81 (d of d, 1 H, *J* = 4.1, 6.5 Hz). ^{13}C NMR (75.4 MHz, 20.8 °C, CD_3NO_2): δ 113.3 (s), 112.4 (s), 103.1 (s), 102.1 (d of d, *J* = 12, 162 Hz), 91.0 (s), 87.9 (d of d, *J* = 6, 163 Hz), 58.7 (t of d, *J* = 161, 8.5 Hz), 56.1 (q of d, *J* = 148, 10 Hz), 55.4 (t of d, *J* = 164, 6 Hz), 48.6 (t of d, *J* = 162, 5 Hz), 28.3 (q, *J* = 127 Hz), 25.9 (q, *J* = 128 Hz), 24.9 (q, *J* = 129 Hz), 22.3 (q, *J* = 129 Hz), 22.0 (q of d, *J* = 128, 6 Hz). $^{31}P\{^1H\}$ NMR (121.4 MHz, 18.1 °C, CD_3NO_2): δ 146.1. Data for the tris(phosphite) adduct are as follows. ^1H NMR (299.9 MHz, CD_3NO_2): δ 5.66 (s, 1 H), 3.72 (br, 27 H), 2.86 (s, 2 H), 2.14 (s, 6 H), 0.99 (s, 2 H). ^{13}C NMR (75.4 MHz, 18.7 °C, CD_3NO_2): δ 123.0 (s), 90.9 (d, *J* = 164 Hz), 55.6 (t, *J* = 161 Hz), 54.2 (q, *J* = 147 Hz), 26.3 (q, *J* = 129 Hz). $^{31}P\{^1H\}$ NMR (121.4 MHz, −20 °C, CD_3NO_2): δ 153.6 (t, 1 P, *J* = 64.5 Hz), 138.9 (d, 2 P, *J* = 64.4 Hz).

[16] Without the exposure to CO, the assumed intermediate $Ru(2,4\text{-}C_7H_{11})(\eta^4\text{-}2,4\text{-}C_7H_{12})(PEt_3)^+$ appears to disproportionate, one of the products seeming to be $Ru(2,4\text{-}C_7H_{11})(PEt_3)_3^+$.

[17] (a) Whitesides, T. H.; Budnik, R. A. *Inorg. Chem.* **1975**, *14*, 664. (b) Werner, H.; Werner, R. *Chem. Ber.* **1984**, *117*, 142.

[18] (a) Ma, H.; Weber, P.; Ziegler, M. L.; Ernst, R. D. *Organometallics* **1987**, *6*, 854. (b) Knox, S. A. R.; Phillips, R. P.; Stone, F. G. A. *J. Chem. Soc., Dalton Trans.* **1976**, 552. (c) Howard, J. A. K.; Knox, S. A. R.; Riera, V.; Sosinisky, B. A.; Stone, F. G. A.; Woodward, P. *J. Chem. Soc., Chem. Commun.* **1974**, 673. (d) Williams, G. M.; Fisher, R. A.; Heyn, R. H. *Organometallics* **1986**, *5*, 818. (e) Werner, H.; Werner, R.; Burschka, C. *Chem. Ber.* **1984**, *117*, 152.

[19] Newbound, T. D.; Freeman, J. W.; Wilson, D. R.; Kralik, M. S.; Patton, A. T.; Campana, C. F.; Ernst, R. D. *Organometallics* **1987**, *6*, 2432.

have also been made for related cyclic species (cyclohexadienyl, etc.).[20] For M(dienyl)$(PR_3)_x(CO)_{3-x}$ complexes, limited information is available, except for cyclohexadienyl compounds, and even that is somewhat equivocal. Thus, in some manganese complexes mixtures of symmetric and unsymmetric conformers were often observed, and both steric and electronic arguments were invoked.[17a] It is notable, however, that observed trends in these cyclized complexes do not necessarily carry over to their acyclic dienyl analogues. For example, Re(cyclohexadienyl)$(H)_2(P(C_6H_5)_3)_2$ (VI) has been found to have its hydride ligands located under C3 and under the open edge of the dienyl ligand,[21] while in Re(2,4-C_7H_{11})$(H)_2(P(C_6H_5)_3)_2$ (VII) the phosphine ligands are found in those locations instead (vide infra).[22] Apparently, for the cyclohexadienyl complexes, additional steric repulsions are encountered by the ligand under the open dienyl edge site as a result of the bridging unit and of the shorter C1- - -C5 separation it induces.

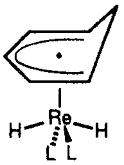

VI

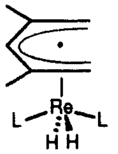

VII

For the Ru(2,4-C_7H_{11})$(PEt_3)_x(CO)_{3-x}$ species (x = 1, 2) variable-temperature ^1H NMR studies indicate that conformations are adopted in which the PEt_3 ligand preferentially resides under the pentadienyl open edge, as in VIII and IX. Hence, phosphine ligands exhibit a greater preference relative to CO for residing in the site under the open pentadienyl edge, in accord with structural results, which indicate that M–P bond lengths are significantly different for the two sites,[19] whereas M–CO distances tend to be more similar.[18a] Thus, the preference for the open site seems to fall in the order PR_3 > CO > halide, which could be related to the relative tendencies of these ligands to withdraw electron density from the metal center. However, as both σ and π interactions are involved, more detailed theoretical studies are clearly warranted. For the unsymmetric Ru(2,4-C_7H_{11})$(PEt_3)_2(CO)^+$, pentadienyl oscillation could not be observed on the NMR time scale up to 96 °C (300 MHz), although significant line broadening was occurring. These data suggest a barrier to oscillation (ΔG^*) of ≥18 kcal/mol. In contrast, for Ru(2,4-C_7H_{11})$(PMe_3)_3^+$, a lower barrier was found of 14.9 ± 0.1 kcal/mol.

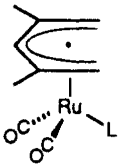

VIII

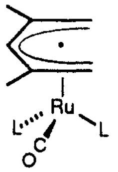

IX

Structural Results and Discussion

A structural study was undertaken for Os(C_5H_5)(2,4-C_7H_{11}) in order to allow for a comparison to the related iron and ruthenium species. Not surprisingly, the osmium compound was found to be isomorphous with its lighter relatives, although some notable structural differences were found (vide infra). Pertinent bonding parameters may be found in Tables II and III, and a structural plot can be seen in Figure 3. While the iron and ruthenium compounds exist in the eclipsed conformation in the solid state,[10,23] the structural result for osmium indicates that both the eclipsed and the staggered conformations are present in ca. a 3:2 ratio, due to the cyclopentadienyl ligand occupying two sites. The Os–C(pentadienyl) distances are all similar, averaging 2.205 (6) Å, which seems slightly shorter than

Table II. Positional Coordinates for the Non-Hydrogen Atoms of Os(C_5H_5)(2,4-C_7H_{11})

atom	x	y	z	U(equiv), Å^2
Os	0.13700 (9)	0.75000 (0)	0.50358 (3)	0.0235 (2)
C1	−0.086 (2)	0.6420 (12)	0.5801 (8)	0.037 (4)
C2	0.129 (2)	0.6490 (10)	0.6342 (7)	0.031 (4)
C3	0.218 (3)	0.7500 (0)	0.6653 (10)	0.031 (5)
C4	0.277 (3)	0.5562 (10)	0.6506 (9)	0.042 (4)
C5	0.449 (5)	0.7500 (0)	0.4121 (20)	0.032 (7)
C6	0.330 (4)	0.6589 (21)	0.3890 (15)	0.038 (6)
C7	0.109 (4)	0.6932 (18)	0.3462 (14)	0.034 (6)
C51	0.428 (6)	0.6967 (26)	0.4030 (22)	0.027 (9)
C61	0.238 (6)	0.6592 (28)	0.3700 (21)	0.024 (9)
C71	0.070 (10)	0.7500 (0)	0.3381 (38)	0.036 (14)

Table III. Pertinent Bond Distances (Å) and Angles (deg) for Os(C_5H_5)(2,4-C_7H_{11})

		Bond Distances			
Os–C1	2.190 (14)	Os–C5	2.216 (31)	Os–C51	2.30 (3)
Os–C2	2.205 (11)	Os–C6	2.260 (23)	Os–C61	2.24 (3)
Os–C3	2.235 (14)	Os–C7	2.258 (19)	Os–C71	2.27 (5)
C1–C2	1.464 (17)	C5–C6	1.42 (3)	C51–C61	1.30 (5)
C2–C3	1.484 (15)	C6–C7	1.49 (3)	C61–C71	1.61 (6)
C2–C4	1.513 (19)	C7–C7′	1.49 (5)	C51–C51	1.40 (7)
		Bond Angles			
C1–C2–C3	120.2 (12)	C6–C5–C6′	114 (3)		
C2–C3–C2′	126.0 (15)	C6–C7–C7′	107.5 (14)		
C1–C2–C4	121.5 (12)	C51–C61–C71	110 (3)		
C3–C2–C4	117.9 (12)	C61–C71–C61′	95 (4)		
C5–C6–C7	105 (2)	C51–C61–C71′	110 (3)		

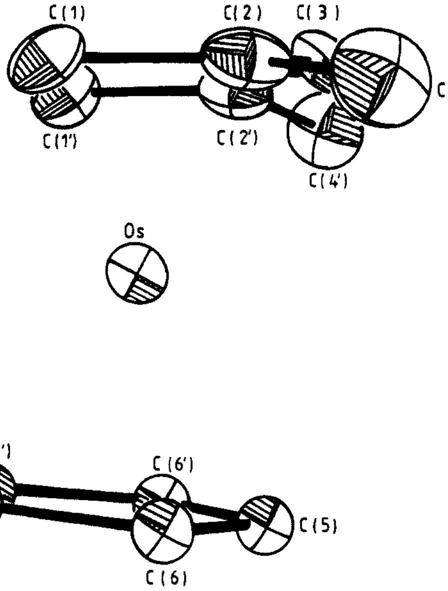

Figure 3. Perspective view and numbering scheme for Os(C_5H_5)(2,4-C_7H_{11}), illustrating the predominant form. A crystallographic mirror plane is present.

---

(20) Ashworth, T. V.; Chalmers, A. A.; Liles, D. C.; Meintjies, E.; Singleton, E. *Organometallics* **1987**, *6*, 1543.

(21) Baudry, D.; Ephritikhine, M.; Felkin, H.; Jeannin, Y.; Robert, F. *J. Organomet. Chem.* **1981**, *220*, C7.

(22) Waldman, T.; Rheingold, A. L.; Ernst, R. D. *J. Organomet. Chem.*, in press.

(23) Wilson, D. R.; Kralik, M. S.; Arif, A. M.; Ernst, R. D. Unpublished results.

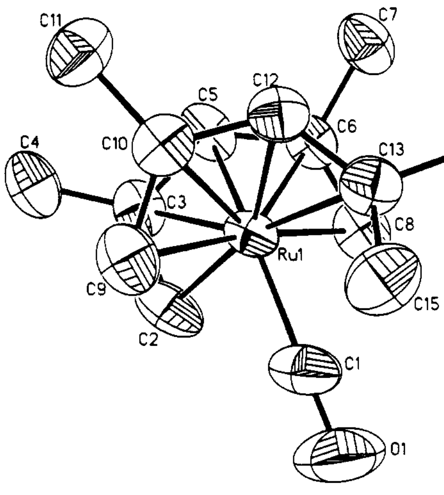

Figure 4. Molecular structure of Ru(η^5-2,4-C_7H_{11})(η^4-2,4-C_7H_{12})(CO)$^+$.

Table IV. Positional Parameters for the Non-Hydrogen Atoms of Ru(2,4-C_7H_{11})(2,4-C_7H_{12})(CO)$^+BF_4^-$

atom[a]	x	y	z	U(equiv), Å^2
Ru	0.13929 (8)	0.73858 (3)	0.99240 (4)	0.0432 (2)
O	0.4704 (7)	0.7933 (5)	1.1147 (4)	0.112 (3)
C1	0.3443 (9)	0.7762 (5)	1.0675 (5)	0.067 (3)
C2	0.1117 (10)	0.6571 (5)	1.1116 (5)	0.071 (4)
C3	−0.0379 (10)	0.6464 (5)	1.0430 (5)	0.055 (3)
C4	−0.1948 (10)	0.6765 (6)	1.0628 (5)	0.074 (4)
C5	−0.0393 (9)	0.6154 (4)	0.9533 (5)	0.054 (3)
C6	0.1010 (9)	0.5954 (4)	0.9190 (5)	0.050 (3)
C7	0.0615 (10)	0.5807 (5)	0.8166 (5)	0.066 (3)
C8	0.2650 (10)	0.5993 (5)	0.9713 (5)	0.063 (4)
C9	0.0399 (10)	0.8803 (5)	1.0276 (5)	0.063 (3)
C10	−0.0339 (9)	0.8584 (4)	0.9341 (5)	0.050 (3)
C11	−0.2190 (9)	0.8495 (6)	0.9008 (5)	0.067 (4)
C12	0.0611 (8)	0.8330 (4)	0.8722 (4)	0.047 (3)
C13	0.2315 (9)	0.8420 (5)	0.8874 (5)	0.053 (3)
C14	0.3128 (10)	0.7939 (5)	0.8223 (5)	0.069 (4)
C15	0.3317 (9)	0.9289 (5)	0.9319 (5)	0.069 (4)
B	−0.0407 (16)	0.0595 (10)	0.7265 (9)	0.095 (4)
F1	0.1030 (7)	0.0813 (4)	0.7852 (4)	0.107 (2)
F2*	−0.0674 (17)	0.0777 (12)	0.6350 (9)	0.046 (3)
F3*	−0.1034 (18)	0.1597 (11)	0.7232 (10)	0.098 (5)
F4*	0.0285 (18)	−0.0362 (10)	0.6941 (10)	0.091 (5)
F5*	−0.0322 (30)	0.0242 (19)	0.6528 (18)	0.151 (9)
F6*	−0.0766 (18)	0.1196 (11)	0.6526 (10)	0.066 (5)
F7*	−0.1306 (15)	−0.0073 (8)	0.7472 (8)	0.108 (4)
F8*	−0.1592 (26)	0.1405 (16)	0.7512 (14)	0.157 (8)
F9*	−0.1608 (15)	0.0296 (9)	0.7693 (8)	0.085 (4)

[a] The fluorine atoms marked by an asterisk were subject to disorder and assigned occupancy factors of 0.33, except for F7 (0.53) and F9 (0.46).

the values of 2.250 (10) and 2.270 (16) Å, respectively, for the eclipsed and staggered cyclopentadienyl images. For the ruthenium analogue, a similar trend was observed, 2.168 (3) vs 2.178 (3) Å. While most of the ligand parameters are not well defined, a few do merit note. As generally observed, the presence of a methyl group on C2 leads to a smaller C1–C2–C3 angle relative to C2–C3–C2′, 120.2 (12)° vs 126.0 (15)°.[24] The methyl group is located 0.30 Å below the pentadienyl least-squares plane, corresponding to a tilt of 11.5°.[25] Such tilts have been ascribed to an attempt by the dienyl ligand to point its p orbitals more toward the metal center.[24,26] The angles formed between the five-membered pentadienyl plane and the two cyclopentadienyl ligand images are 7.6 and 9.0°, respectively.

Table V. Pertinent Bond Distances (Å) and Angles (deg) for Ru(2,4-C_7H_{11})(2,4-C_7H_{12})(CO)$^+BF_4^-$

Bond Distances					
Ru–C1	1.887 (7)	C2–C3	1.426 (10)	C1–O	1.147 (9)
Ru–C2	2.196 (7)	C3–C5	1.428 (10)	B–F1	1.344 (13)
Ru–C3	2.244 (8)	C5–C6	1.435 (11)	B–F2	1.38 (2)
Ru–C5	2.251 (7)	C6–C8	1.410 (10)	B–F3	1.48 (2)
Ru–C6	2.254 (6)	C3–C4	1.489 (12)	B–F4	1.57 (2)
Ru–C8	2.259 (7)	C6–C7	1.521 (9)	B–F5	1.24 (3)
Ru–C9	2.248 (7)	C9–C10	1.432 (9)	B–F6	1.37 (2)
Ru–C10	2.236 (6)	C10–C12	1.427 (11)	B–F7	1.28 (2)
Ru–C12	2.205 (6)	C12–C13	1.403 (10)	B–F8	1.61 (3)
Ru–C13	2.414 (7)	C13–C15	1.524 (9)	B–F9	1.40 (2)
		C10–C11	1.519 (10)	C13–C14	1.494 (12)

Bond Angles			
C2–C3–C5	121.3 (7)	C9–C10–C12	122.1 (6)
C3–C5–C6	126.7 (6)	C10–C12–C13	126.4 (6)
C5–C6–C8	124.7 (6)	C12–C13–C15	124.9 (6)
C2–C3–C4	119.4 (7)	C9–C10–C11	119.9 (7)
C4–C3–C5	119.0 (6)	C11–C10–C12	117.6 (6)
C5–C6–C7	114.2 (6)	C12–C13–C14	118.3 (6)
C7–C6–C8	120.7 (7)	C14–C13–C15	110.4 (7)
Ru–C1–O	175.8 (7)		

The structure of Ru(2,4-C_7H_{11})(η^4-2,4-C_7H_{12})(CO)$^+$ may be seen in Figure 4, and bonding parameters are listed in Tables IV and V. Relative to the mixed carbonyl phosphine discussion, the conformation of this species may be regarded as symmetric. However, in this case it is the better accepting ligand that is located by the open dienyl edge. Quite possibly this occurs as a result of the tilt experienced by the unique edge site. A chelating 1,3-diene would clearly be better able to span the two nonedge sites rather than the edge and a nonedge site. The resulting symmetric structure may also then be considered as a hybrid of the syn-eclipsed M(dienyl)$_2$L and M(diene)$_2$L species (X and XI).[24] Related iron compounds possessing

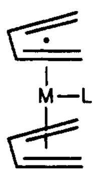

X

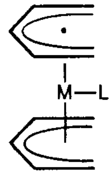

XI

cyclohexadienyl, cycloheptadienyl, and cyclooctadienyl ligands are known and presumably possess similar structures.[27]

The structural data suggest that significant steric crowding is present. Thus, the Ru–C8 distance of 2.259(7) Å is somewhat longer than the Ru–C2 distance of 2.196 (7) Å, which may be attributed to the location of C9 near the congested end of the C_7H_{12} ligand. Similarly, the Ru–C13 distance of 2.414 (7) Å is notably longer than the Ru–C9 distance of 2.248 (7) Å. The pentadienyl methyl groups display the usual deformations from the five-membered plane, in that C4 and C7 are located 0.165 and 0.223 Å out of the plane in a direction toward the metal atom, corresponding to respective tilts of 6.4 and 8.4°. A similar tilt from the butadiene plane of 0.389 Å (15.1°) is observed for C14, whereas C11 and C15 experience opposite displacements (away from the metal) by −0.053 and

---

(24) Ernst, R. D. *Struct. Bonding (Berlin)* **1984**, *57*, 1.

(25) For a given substituent attached to a pentadienyl atom X, the sine of the tilt angle θ is defined as the displacement of a given atom from the least-squares plane divided by the distance between this atom and atom X.

(26) (a) Elian, M.; Chen, M. M. L.; Mingos, D. M. P.; Hoffmann, R. *Inorg. Chem.* **1976**, *15*, 1148. (b) Haaland, A. *Acc. Chem. Res.* **1979**, *12*, 415.

(27) (a) Johnson, B. F. G.; Lewis, J.; Matheson, T. W.; Ryder, I. E.; Twigg, M. V. *J. Chem. Soc., Chem. Commun.* **1974**, 269. (b) Ashley-Smith, J.; Howe, D. V.; Johnson, B. F. G.; Lewis, J.; Ryder, I. E. *J. Organomet. Chem.* **1974**, *82*, 257.

Table VI. Positional Coordinates for the Non-Hydrogen Atoms of $Ru(2,4\text{-}C_7H_{11})(CO)_2(PEt_3)^+BF_4^-$

atom[a]	*x*	*y*	*z*	*U*(equiv), Å^2
Ru	0.14133 (5)	0.2500	0.27801 (5)	0.0338 (1)
P	0.32396 (16)	0.2500	0.15675 (16)	0.0373 (5)
C1	−0.0282 (4)	0.1323 (3)	0.1088 (4)	0.046 (2)
C2	−0.0862 (4)	0.1454 (3)	0.2221 (4)	0.041 (1)
C3	−0.1162 (6)	0.2500	0.2708 (6)	0.041 (2)
C4	−0.1011 (5)	0.0471 (3)	0.3100 (5)	0.060 (2)
C5	0.2630 (4)	0.1414 (4)	0.4195 (4)	0.050 (2)
C6	0.2221 (7)	0.2500	−0.0444 (6)	0.052 (3)
C7	0.3294 (9)	0.2500	−0.1358 (8)	0.078 (4)
C8	0.4658 (4)	0.1342 (3)	0.2011 (5)	0.049 (2)
C9	0.3849 (5)	0.0230 (3)	0.1520 (5)	0.064 (2)
O	0.3326 (4)	0.0780 (3)	0.5040 (4)	0.083 (2)
B	0.7763 (14)	0.2500	0.6536 (10)	0.071 (4)
F1	0.6420 (8)	0.2500	0.5411 (6)	0.192 (4)
F2	0.8319 (11)	0.1634 (8)	0.7393 (9)	0.133 (4)
F3*	0.9125 (23)	0.2500	0.6072 (16)	0.206 (13)
F4*	0.7252 (18)	0.2500	0.7633 (12)	0.166 (9)
F5	0.8278 (15)	0.1571 (9)	0.6335 (17)	0.260 (11)

[a] The fluorine atoms with an asterisk have occupancy factors of 0.25; the other fluorine atoms have occupancy factors of 0.50.

Table VII. Pertinent Bond Distances (Å) and Angles (deg) for $Ru(2,4\text{-}C_7H_{11})(CO)_2(PEt_3)^+BF_4^-$

Bond Distances

Ru–P	2.353 (2)	C1–C2	1.404 (6)	B–F1	1.268 (10)
Ru–C1	2.267 (3)	C2–C3	1.428 (5)	B–F2	1.323 (10)
Ru–C2	2.269 (4)	C2–C4	1.515 (6)	B–F3	1.447 (26)
Ru–C3	2.256 (6)	P–C6	1.819 (5)	B–F4	1.319 (20)
Ru–C5	1.920 (4)	P–C8	1.832 (4)	B–F5	1.269 (13)
C5–O	1.127 (5)	C6–C7	1.541 (11)	C8–C9	1.526 (5)

Bond Angles

C5–Ru–C5′	87.6 (2)	C1–C2–C3	122.7 (4)
C5–Ru–P	93.5 (1)	C2–C3–C2′	127.6 (6)
C3–Ru–P	150.6 (1)	C1–C2–C4	120.0 (4)
C1–Ru–C5	173.5 (2)	C3–C2–C4	117.0 (4)
Ru–C5–O	178.7 (4)	P–C6–C7	118.2 (4)
Ru–P–C6	113.5 (2)	P–C8–C9	114.9 (3)
Ru–P–C8	115.1 (2)		

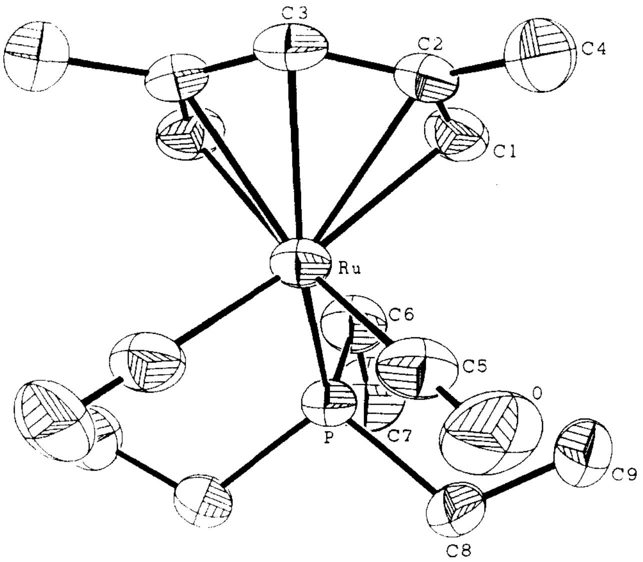

Figure 5. Perspective view of $Ru(2,4\text{-}C_7H_{11})(CO)_2(PEt_3)^+$, illustrating the crystallographic mirror plane symmetry.

Table VIII. Positional Coordinates for the Non-Hydrogen Atoms of $Ru(2,4\text{-}C_7H_{11})(CO)(PEt_3)_2{}^+BF_4^-$

atom	*x*	*y*	*z*	*U*(equiv), Å^2
Ru	0.40053 (14)	0.14795 (5)	0.01572 (13)	0.0438 (5)
P1	0.5184 (4)	0.14618 (18)	−0.1220 (4)	0.051 (2)
P2	0.1939 (4)	0.11207 (16)	−0.1451 (4)	0.050 (2)
C1	0.3544 (16)	0.2290 (5)	−0.0310 (13)	0.066 (10)
C2	0.2867 (16)	0.2143 (6)	0.0474 (15)	0.057 (9)
C3	0.3444 (17)	0.1878 (6)	0.1683 (16)	0.067 (11)
C4	0.4864 (18)	0.1716 (6)	0.2321 (16)	0.067 (10)
C5	0.5834 (14)	0.1842 (5)	0.1846 (13)	0.064 (9)
C6	0.1358 (15)	0.2246 (6)	0.0042 (18)	0.088 (12)
C7	0.5337 (19)	0.1358 (6)	0.3566 (13)	0.095 (11)
C8	0.4483 (17)	0.0826 (6)	0.0743 (15)	0.060 (9)
C9	0.4261 (14)	0.1538 (6)	−0.3069 (13)	0.072 (9)
C10	0.3753 (16)	0.2068 (6)	−0.3506 (15)	0.095 (11)
C11	0.6040 (15)	0.0866 (6)	−0.1250 (15)	0.084 (10)
C12	0.7202 (17)	0.0762 (6)	0.0044 (16)	0.10 (1)
C13	0.6550 (14)	0.1924 (5)	−0.0760 (14)	0.060 (9)
C14	0.7378 (16)	0.1928 (7)	−0.1607 (17)	0.086 (12)
C15	0.0724 (15)	0.0944 (5)	−0.0716 (14)	0.056 (9)
C16	0.1316 (18)	0.0605 (6)	0.0513 (16)	0.082 (12)
C17	0.2224 (14)	0.0534 (5)	−0.2134 (14)	0.064 (9)
C18	0.0982 (17)	0.0244 (7)	−0.3102 (20)	0.12 (1)
C19	0.0897 (14)	0.1497 (6)	−0.2978 (13)	0.071 (9)
C20	−0.0656 (13)	0.1425 (7)	−0.3669 (15)	0.084 (10)
O	0.4797 (13)	0.0438 (4)	0.1180 (12)	0.089 (8)
B	0.0377 (26)	0.1454 (10)	0.3073 (19)	0.13 (1)
F1	0.0012 (13)	0.1551 (6)	0.1829 (11)	0.18 (1)
F2	0.0144 (17)	0.1833 (5)	0.3746 (13)	0.22 (1)
F3	0.1680 (16)	0.1454 (11)	0.3618 (16)	0.32 (2)
F4	0.0044 (26)	0.1089 (6)	0.3410 (17)	0.27 (2)

Table IX. Pertinent Bond Distances (Å) and Angles (deg) for $Ru(2,4\text{-}C_7H_{11})(CO)(PEt_3)_2{}^+BF_4^-$

Bond Distances

Ru–C1	2.266 (13)	C1–C2	1.40 (3)	P1–C9	1.834 (13)
Ru–C2	2.289 (18)	C2–C3	1.39 (2)	P1–C11	1.870 (17)
Ru–C3	2.271 (20)	C3–C4	1.46 (2)	P1–C13	1.836 (15)
Ru–C4	2.223 (16)	C4–C5	1.39 (3)	P2–C15	1.870 (19)
Ru–C5	2.266 (12)	C2–C6	1.52 (2)	P2–C17	1.837 (15)
Ru–C8	1.881 (17)	C4–C7	1.56 (2)	P2–C19	1.862 (13)
Ru–P1	2.347 (5)	C8–O	1.14 (2)	B–F1	1.26 (2)
Ru–P2	2.376 (4)	C9–C10	1.54 (2)	B–F2	1.35 (3)
C11–C12	1.46 (2)	C13–C14	1.54 (3)	B–F3	1.27 (3)
C15–C16	1.52 (2)	C17–C18	1.52 (2)	B–F4	1.17 (3)
C19–C20	1.53 (2)				

Bond Angles

P1–Ru–P2	96.7 (2)	C1–C2–C3	125.8 (16)
P1–Ru–C8	93.0 (6)	C2–C3–C4	124.1 (19)
P2–Ru–C8	84.1 (4)	C3–C4–C5	123.8 (15)
P1–Ru–C3	149.9 (5)	C1–C2–C6	122.2 (13)
P2–Ru–C5	173.0 (5)	C3–C2–C6	112.0 (17)
C8–Ru–C1	173.9 (6)	C3–C4–C7	119.1 (18)
Ru–C8–O	175.7 (14)	C5–C4–C7	117.0 (15)
Ru–P1–C9	120.6 (6)	P1–C9–C10	113.5 (10)
Ru–P1–C11	115.9 (6)	P1–C11–C12	112.3 (12)
Ru–P1–C13	113.9 (6)	P1–C13–C14	116.6 (11)
Ru–P2–C15	113.6 (4)	P2–C15–C16	115.1 (12)
Ru–P2–C17	112.6 (5)	P2–C17–C18	118.5 (12)
Ru–P2–C19	116.8 (5)	P2–C19–C20	119.0 (12)
F1–B–F2	112 (2)	F2–B–F3	100 (2)
F1–B–F3	106 (2)	F2–B–F4	109 (3)
F1–B–F4	121 (2)	F3–B–F4	107 (2)

−0.996 Å, corresponding to tilts of −2.0 and −40.8°, respectively.

The structures of $Ru(2,4\text{-}C_7H_{11})(CO)_2(PEt_3)^+$ (VIII) and $Ru(2,4\text{-}C_7H_{11})(CO)(PEt_3)_2{}^+$ (IX) may be best considered together. Bonding parameters may be found in Tables VI–IX, and ORTEP views are presented in Figures 5 and 6. In general, there is little difference between similar portions of these complexes. It can first be noted that in both cases it is a phosphine ligand that resides by the open pentadienyl edge, and these Ru–P distances are 2.353 (2) and 2.347 (5) Å, respectively, for VIII and IX. The M–P distance involving the phosphine ligand under the formally uncharged carbon atom in IX is longer at 2.376 (4) Å. Hence, as with other unsymmetric complexes such as $Cr(2,4\text{-}C_7H_{11})(Cl)(dmpe)$ and $Fe(2,4\text{-}C_7H_{11})(I)(CO)_2$, the metal–ligand bonding appears enhanced when the ligand

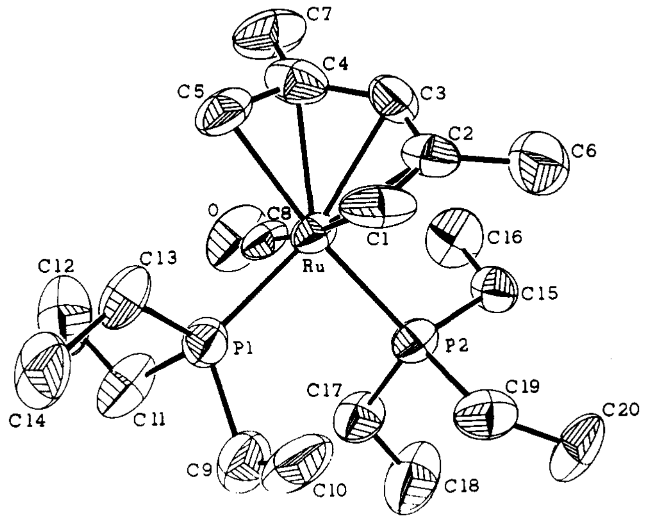

Figure 6. Perspective view of the structure of $Ru(2,4-C_7H_{11})(CO)(PEt_3)_2^+$.

occupies the site under the open edge. However, the enhancement seems more pronounced for phosphine ligands relative to carbonyls. Thus, in $Fe(2,4-C_7H_{11})(I)(CO)_2$, the two Fe–CO distances are 1.774 (7) and 1.786 (6) Å, respectively. It appears, therefore, that the phosphines have more to gain by occupying an edge site than would a carbonyl, and apparently as a direct result of this, when the two ligands are found together, it is indeed the phosphine that occupies the edge site, leading to the observed symmetric and unsymmetric orientations for VIII and IX. Notably, these preferences do not carry over entirely to cyclic relatives such as $M(cyclohexadienyl)(CO)_x[P(OCH_2)_3CEt]_{3-x}$ or $M(cycloheptadienyl)(CO)_x[P(OCH_2)_3CEt]_{3-x}$ ($M = Mn, Re, Fe^+, Ru^+$).[3a,17a] Presumably the presence of the bridge across the pentadienyl unit leads to increased steric encumbrance by the "edge" site, which then diminishes the preference for this site exhibited by the bulkier phosphine ligand. Related situations also occur for $M(dienyl)(L)_4$ and $M(dienyl)(L)_2$ species. Thus, as noted before, $Re(C_6H_7)(H)_2(P(C_6H_5)_3)_2$[21] has been found to adopt structure VI, while $Re(2,4-C_7H_{11})(H)_2(P(C_6H_5)_3)_2$[22] adopts structure VII. Similarly, $Rh(dienyl)(L)_2$ complexes of types XII and XIII have been found.[28]

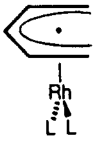

XII

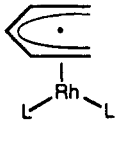

XIII

The principal effect responsible for favoring the edge site appears to be electronic, in that the presence of the open pentadienyl edge seems to make available extra metal orbital density in that vicinity, leading to an upward tilt by the edge ligand, as in V (vide supra). The extent of this tilt may readily be seen by comparing the angles formed between the (five-atom) pentadienyl plane perpendiculars and the Ru–L vectors. For VIII, the angles involving C5 and P are 131.3 and 108.9°, while for IX, the angles involving C8 and P1 are 130.7 and 107.8°, respectively. Hence, tilts of ca. 22.6° are observed. Additionally, as a result of these tilts, the edge-situated ligands move away from a trans orientation relative to the central pentadienyl carbon atoms (e.g., note ∠P1–Ru–C3 = 150.6 (1)° vs ∠C1–Ru–C5 = 173.5 (2)° for VIII). This may also lead to an increase in M–L bond strength for edge-situated ligands.

Some evidence for the greater importance of electronic rather than steric influences in determining these preferences may be gained from the conformations adopted by the PEt_3 ligands. As noted earlier,[29] the smallest attainable form for such a ligand appears to be that of XIV.

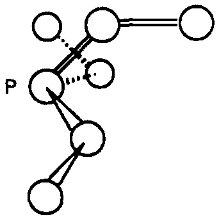

XIV

It can be noted that, in both VIII and IX, the PEt_3 ligands in the edge sites have adopted just this orientation, whereas the PEt_3 ligand under C15 in IX seems to have adopted a more open form. It appears, therefore, that the ligand occupying the edge site encounters greater steric crowding than do ligands in the other two sites. That PEt_3, rather than the smaller CO, would preferentially occupy the more sterically demanding edge site clearly indicates that electronic influences are predominantly responsible for determining the conformations of these species. However, in the bridged analogues (cyclohexadienyl etc.), additional steric interactions are present for the edge site, so that both steric and electronic factors contribute to the observed conformational preferences. Additionally, secondary steric influences are apparently manifested in $Ru(C_5H_7)(PMe_3)(P(C_6H_5)_3)(CO)^+$ and related complexes, for which it is the smaller phosphine ligand that occupies the site under the open dienyl edge.[30]

The bonding parameters for the $2,4-C_7H_{11}$ ligands themselves are similar to those observed in many other such species and require only a few comments. It is notable that the Ru–C bond distances seem quite constant for the two structures. Thus, in VIII, the Ru–C distances involving carbon atoms in the 1,5-, 2,4- and 3-positions are 2.267 (3), 2.269 (4), and 2.256 (6) Å, while the corresponding average Ru–C distances in IX are 2.266 (9), 2.256 (12), and 2.271 (20) Å, respectively. The methyl groups in the symmetric dicarbonyl complex are located 0.216 Å below the pentadienyl ligand plane, corresponding to a tilt of 8.2°. For the unsymmetric monocarbonyl, a similar displacement of 0.251 Å (9.2° tilt) is observed for C19. However, C16 is displaced *away from* the metal atom by 0.026 Å (−1.0° tilt), which can be attributed to its eclipsing interaction with one of the phosphine ligands.

Conclusions

The protonated open ruthenocene "$HRu(2,4-C_7H_{11})_2^+$" serves as a convenient precursor for the preparation of $Ru(2,4-C_7H_{11})(L)_2(L')^+$ species. The latter ions exhibit distinct conformational preferences as a result of electronic differences between the three ligand sites. In general, good donor ligands seem to prefer the sites under the open pentadienyl edge, while one-electron ligands tend to reside in the other positions. Thus far, it appears likely that all ligands actually favor the edge site, and therefore the observed conformations are dictated by the ligand having the

---

[28] (a) Dahlenburg, L.; Höck, N. *J. Organomet. Chem.* **1985**, *284*, 129. (b) Cetinkaya, B.; Hitchcock, P. B.; Lappert, M. F.; Torroni, S.; Atwood, J. L.; Hunter, W. E.; Zaworotko, M. J. *J. Organomet. Chem.* **1980**, *188*, C31.

[29] Stahl, L.; Ernst, R. D. *J. Am. Chem. Soc.* **1987**, *109*, 5673.

[30] Bleeke, J. R.; Rauscher, D. J. *J. Am. Chem. Soc.* **1989**, *111*, 8972.

greatest preference. However, the presence of significant steric interactions can also lead to additional variations in preferences, notably for cyclic dienyl species, and further studies will be required to better understand the extent of these contributions.

Acknowledgment. R.D.E. is grateful to the National Science Foundation for support of this work and to Prof. John Gladysz for helpful discussions.

Supplementary Material Available: Tables of thermal and hydrogen atom parameters, least-squares plane data, and atomic parameters for the atoms in $Os(C_5H_5)(2,4\text{-}C_7H_{11})$, $Ru(2,4\text{-}C_7H_{11})(2,4\text{-}C_7H_{12})(CO)^+BF_4^-$, $Ru(2,4\text{-}C_7H_{11})(CO)_2(PEt_3)^+BF_4^-$, $Ru(2,4\text{-}C_7H_{11})(CO)(PEt_3)_2^+BF_4^-$, and "$HRu(2,4\text{-}C_7H_{11})_2^+BF_4^-$" (12 pages); tables of structure factors (53 pages). Ordering information is given on any current masthead page.

Diastereoselective Ligand and Vertex Substitutions in Bimetallic Bridged Alkyne Clusters: X-ray Crystal Structure of (μ_2-*endo*-2-Propynylborneol)hexacarbonyldicobalt

Michael F. D'Agostino, Christopher S. Frampton, and Michael J. McGlinchey*

Department of Chemistry, McMaster University, Hamilton, Ontario, Canada L8S 4M1

Received November 27, 1989

Enantiomerically pure dicobalt μ-alkyne clusters that possess diastereotopic $Co(CO)_3$ vertices can be synthesized by the treatment of (propargyl alcohol)$Co_2(CO)_6$ with menthol or borneol or by the reaction of $Co_2(CO)_8$ with *endo*-2-propynylborneol. Ligand substitution reactions with phosphines occur with some degree of diastereoselectivity to give mixtures of monosubstituted complexes. Moreover, diastereoselective replacement of a metal vertex by isolobal groups, $(C_5H_4R)M(CO)_2$, where M = Mo, W, has been observed. The hexacarbonyldicobalt complex, **6**, of *endo*-2-propynylborneol has been synthesized and characterized by X-ray crystallography. The crystals are orthorhombic of space group $P2_12_12_1$ with a = 12.136 (3) Å, b = 12.682 (2) Å, c = 13.652 (3) Å, V = 2101 (1) Å^3, D_c = 1.51 g cm^{-3}, and D_m = 1.49 g cm^{-3} for Z = 4 and R_1 = 0.0546 and R_2 = 0.0567 for 3713 unique reflections (R_1 = 0.0437 and R_2 = 0.0463 for 2953 reflections with $I > 2.5\sigma(I)$).

Introduction

It has been recently reported that mixed metal clusters, such as 1, that bear a chiral substituent derived from a natural product are readily synthesizable on the multigram scale.[1,2] In these molecules, the two tricarbonylcobalt vertices are rendered diastereotopic and so, in principle, should be differently susceptible to attack by incoming ligands. Indeed, we have shown that use of bulky phosphines can lead to a small degree of chiral discrimination. The diastereotopic character of these vertices was readily demonstrated by the incorporation of a bidentate ligand, e.g., $Ph_2PCH_2CH_2PPh_2$, yielding 2, which exhibited two distinct phosphorus resonances in the ^{31}P NMR spectrum.[1] Moreover, a recent note from Nicholas' laboratory[3] describes elegant work whereby reaction of triphenylphosphine with a racemic mixture of chiral (propargyl alcohol)$Co_2(CO)_6$ clusters leads to preferential diastereomer formation; this prompts us to report the results of our own studies, which demonstrate the generality of this phenomenon for $(R^*C{\equiv}CR)Co_2(CO)_6$ complexes in which R* is a chiral substituent derived from a natural product.[4]

It is clear that there exists some tendency for preferential attack by an incoming ligand because of the intrinsic diastereotopic nature of the metal vertices. However, one might also envisage an extension of this concept to include the direct replacement of only one $Co(CO)_3$ vertex by an isolobal metal fragment, thus generating enantiomerically pure, chiral heterobimetallic clusters without the need to resort to time-consuming diastereomer separations. To this end, we have prepared several enantiomerically pure dicobalt μ-alkyne clusters and examined not only ligand substitutions but also complete vertex replacement processes on these compounds.

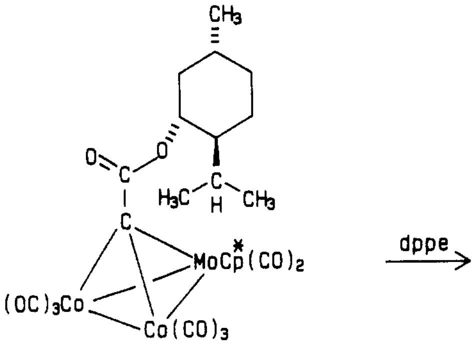

1

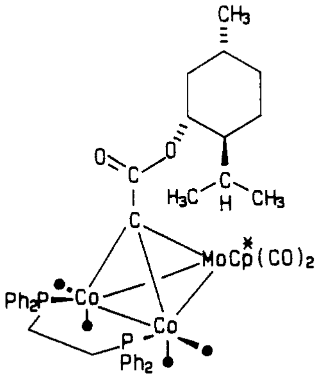

2

---

(1) Clark, D. T.; Sutin, K. A.; McGlinchey, M. J. *Organometallics* **1989**, *8*, 155.

(2) Blumhofer, R.; Vahrenkamp, H. *Chem. Ber.* **1986**, *119*, 683.

(3) Bradley, D. H.; Masood, A. K.; Nicholas, K. M. *Organometallics* **1989**, *8*, 554.

(4) First reported at the Third Chemical Congress of North America, Toronto, Canada, June 4-10, 1988.

0276-7333/90/2309-2972$02.50/0